BIODIVERSITAS
Volume 26, Number 6, June 2025
Pages: 2916-2925

ISSN: 1412-033X
E-ISSN: 2085-4722
DOI: 10.13057/biodiv/d260634

Genome mining, metabolite fractionation, and evaluation of antibiofilm activity of endophytic *Priestia megaterium* AJ5 against methicillin-resistant *Staphylococcus aureus*

JEPRI AGUNG PRIYANTO[1,♥], GENIA SOTYA SINARAWADI[1], MUHAMMAD EKA PRASTYA[2], ORHINTA MUTIARA JATI[1], NISA RACHMANIA[1], ZETRYANA PUTERI TACHRIM[2]

[1]Division of Microbiology, Department of Biology, Faculty of Mathematics and Natural Sciences, Institut Pertanian Bogor. Jl. Agatis, Dramaga, Bogor 16680, West Java, Indonesia. Tel./fax.: +62-251-8622833, ♥email: jepriyanto@apps.ipb.ac.id

[2]Research Center for Pharmaceutical Ingredients and Traditional Medicine, National Research and Innovation Agency. Jl. Raya Jakarta-Bogor Km. 46 Cibinong, Bogor 16911, West Java, Indonesia

Manuscript received: 8 February 2025. Revision accepted: 6 June 2025.

Abstract. *Priyanto JA, Sinarawadi GS, Prastya ME, Jati OM, Rachmania N, Tachrim ZP. 2025. Genome mining, metabolite fractionation, and evaluation of antibiofilm activity of endophytic* Priestia megaterium *AJ5 against Methicillin-resistant* Staphylococcus aureus*. Biodiversitas 26: 2916-2925.* Endophytic bacteria, particularly *Priestia megaterium*, are a source of secondary metabolites that are valuable for medicinal purposes. Therefore, this study aimed to mine the Secondary Metabolite Gene Clusters (SMGCs) within the complete genome of AJ5 strain, fractionate its secondary metabolites, and evaluate its antibiofilm activity against Methicillin-Resistant *Staphylococcus aureus* (MRSA). The bacterium had a complete genome length of 5,750,510 bp and was closely related to *P. megaterium* NCTC10342, with an Average Nucleotide Identity (ANI) of 98.37%. AntiSMASH analysis showed that the bacterium possessed 5 types of SMGCs, including Non-Ribosomal Peptide Synthetase (NRPS)-Independent (NI) siderophores, 3 types of terpenes, and type III Polyketide Synthase (PKS). In addition, 2 selected fractions obtained from thin-layer chromatography and column chromatography procedures exhibited strong anti-MRSA activity. F9 and F12 fractions had Minimum Inhibitory Concentrations (MIC) of 117.5 µg/mL and 180 µg/mL, respectively. Liquid Chromatography-Mass Spectrometry/Mass Spectrometry (LC-MS/MS) analysis indicated that these 2 fractions contained nigakilactone H, tetratriacontanamine, 2-(p-Anisyl)-5-methyl-1-hexene, and other unidentified compounds. The compounds were also capable of suppressing biofilm formation of MRSA by up to 81.54%±1.80 for the F9 and 77.01%±1.96 for F12 fraction after treatment with 1×MIC. All selected fractions also exhibited eradication activity against established MRSA biofilms up to 79.23±1.96%. In conclusion, this study showed the SMGCs profile and their metabolite products found within the genome of AJ5 strain, as well as its antibiofilm potential against MRSA. The thoroughness of our research process and the validity of our findings suggest that genome-based screening and in vitro assays could significantly accelerate the development of novel anti-MRSA agents.

Keywords: *Archidendron pauciflorum*, endophyte, Nigakilactone H, SMGCs, tetratriacontanamine

INTRODUCTION

The incidence of Antimicrobial Resistance (AMR) cases is increasing due to the excessive use of antibiotics in treating public health issues. One of the primary bacterial pathogens associated with the cases is Methicillin-Resistant *Staphylococcus aureus* (MRSA) (Khan et al. 2017). This bacterium is commonly associated with skin and soft tissue infections (Montravers and Eckmann 2021) and responsible for more than 600,000 deaths worldwide in 2019, higher than that of other pathogenic bacteria such as *Streptococcus pneumoniae*, *Klebsiella pneumoniae*, *Pseudomonas aeruginosa*, and *Acinetobacter baumannii* (Murray et al. 2022). In addition, MRSA is generally resistant to β-lactam antibiotics (including oxacillin, penicillin, and methicillin) and cephalosporins (Alghamdi et al. 2023). The bacterium can develop resistance to these antibiotics by acquiring a single genetic element known as the Staphylococcal Cassette Chromosome mec (SCCmec), which produces Penicillin-Binding Protein 2a (PBP2a) (Vestergaard et al. 2019). Various MRSA strains become resistant to β-lactam antibiotics through the acquisition of the *blaZ* gene, which may either integrate into the chromosome or reside on large conjugative plasmids. The gene encodes β-lactamase, which can hydrolyze the essential β-lactam ring (Andrzejczuk et al. 2023). This high prevalence has led to the exploration of new substances to address drug-resistant pathogens, particularly MRSA.

The formation of biofilms by *S. aureus* is another factor contributing to AMR. Biofilms are a structured community of microbial cells that facilitate the attachment of free-floating bacteria to both living and non-living surfaces (Flemming and Wuertz 2019). The community is shielded by an extracellular polymeric matrix primarily made up of oligosaccharides, DNA, and proteins, which significantly enhances bacteria's resistance to drug treatments and contributes to their virulence and chronic pathogenicity. MRSA has emerged as a challenging pathogen due to its biofilm-forming ability (Silva et al. 2021). Consequently, higher concentrations of antibiotics are necessary to eradicate

biofilms compared to planktonic bacteria. To address this issue, there is an urgent need to discover new anti-MRSA agents that not only inhibit the growth of MRSA but also suppress its biofilm formation and eradicate the established biofilm.

A promising alternative that has attracted interest in recent years is endophytes, which are symbiotic microorganisms inhabiting the inner tissues of plants without causing disease (Christina et al. 2013). Among endophytic species, *Priestia megaterium* (formerly known as *Bacillus megaterium*) is one of the most frequently isolated from various plants, such as *Bolboschoenus planiculmis*, *Malus domestica*, *Arachis hypogaea*, and *Solanum tuberosum* (Hwang et al. 2022; Mahmoud et al. 2023; Zhang et al. 2023). The bacterium plays a pivotal role in promoting plant growth and facing environmental stresses (Shi et al. 2023). It can also produce biotechnologically important metabolites, such as bacitracin (Al-Thubiani et al. 2018), daidzein, and genistein (Al-Theyab et al. 2023). The bacterium has also demonstrated remarkable antimicrobial activity against pathogenic microbes (Malanicheva et al. 2012; Cui et al. 2023). Therefore, exploring the secondary metabolites produced by *Priestia* species could be a strategic approach to discovering antibiotics beneficial for medicinal purposes.

In a previous study, the crude extract of bacterial secondary metabolites from AJ5 strain, isolated from the roots of dogfruit (*Archidendron pauciflorum*), exhibited significant antibacterial activity against multidrug-resistant strains (Priyanto et al. 2023). However, the substances responsible for this activity and the complete genomic profile of the isolate remain unidentified. Approaches, such as metabolite fractionation and genome mining may enhance an understanding of the identity of antibacterial or antibiofilm compounds and their potential biosynthetic pathways. Genome sequencing and bioinformatics analysis can also yield insights into the Secondary Metabolite Gene Clusters (SMGCs) present in individual bacteria. The significant impact of recent advancements in sequencing technologies and the affordable access to genomic data facilitate the use of various bioinformatics tools to identify and annotate highly conserved regions of SMGCs (Alberus et al. 2022). Recent studies have focused on large-scale genomic datasets, showing the significant potential for uncovering novel compounds from microorganisms, including *Streptomyces* (Belknap et al. 2020), *Bacillus* (Saikat et al. 2024; Priyanto et al. 2024), *Priestia* (Maghembe et al. 2023), *Paenibacillus* (Kim et al. 2024), and *Pseudomonas* (Tamang et al. 2024). Therefore, this study aimed to mine the genome of *P. megaterium* AJ5 to identify the SMGCs, fractionate its secondary metabolites, and assess its antibiofilm activity against MRSA.

MATERIALS AND METHODS

Strain collection

AJ5 strain used in this study was isolated from the root of *Archidendron pauciflorum* and stored at the Laboratory of Microbiology, Department of Biology, Faculty of Mathematics and Natural Sciences, IPB University, Bogor, Indonesia. 16S-rRNA-based identification revealed that this bacterium belonged to the *Priestia megaterium*. The 16S-rRNA partial sequence (1181 bp) of this bacterium was accessible at https://ncbi.nlm.nih.gov under accession number OP164672.1. In addition, MRSA was obtained from Central General Hospital Dr. Kariadi, Semarang, Central Java, Indonesia.

Procedures

Whole genome sequencing and identification for Secondary Metabolite biosynthetic Gene Clusters (SMGCs)

The bacterial cells from a 24-hour culture were centrifuged at 15,000 rpm for 1 minute. Genomic DNA was isolated using the Quick-DNA Fungal Bacterial Isolation Kit (Zymo Research, California, United States of America), following the kit's instructions. The bacterial genome sequence was obtained through Oxford Nanopore Technology (Cambridge, United Kingdom). De novo assembly was conducted with Flye (v.2.8.3), and following this, mapping and iterative genome polishing were performed 4 times using Minimap2 (v.2.24-r1122) and Racon (v.1.5.0). The completeness of the assembled sequence and related species' genomes was evaluated using fast-qc (v.0.4.2) and BUSCO (v.5.4.4). Quality assessment of the assembled sequence was carried out using Quast software (v.5.0.2). The bacterial genome was visualized using Circos (v.0.69-8). Furthermore, antiSMASH version 7.1.0 was used to annotate SMGCs in the bacterial genome (https://antismash.secondarymetabolites.org) (Blin et al. 2023), and complete genome sequences of *P. megaterium* AJ5 were deposited to NCBI Genbank database (https://submit.ncbi.nlm.nih.gov/about/genome).

Culture and extraction of secondary metabolites

AJ5 strain was grown in 2 L of Nutrient Broth (NB) medium (Oxoid, England), agitated at 120 rpm, and incubated for 72 hours. The culture was then equally added with ethyl acetate and shaken continuously for 20 minutes. Subsequently, the upper layer was then separated and concentrated using a rotary evaporator at 50°C. The culture was extracted twice with the same solvent, and the concentrated extract was then collected (Priyanto et al. 2023).

Thin Layer Chromatography (TLC)

A total of 2 mg of crude extract from the AJ5 strain was diluted in methanol. This suspension was applied to a Thin Layer Chromatography (TLC) plate coated with silica gel 60 F_{254} (Merck, Darmstadt, Germany) using a capillary tube and then allowed to air dry. The TLC plate was subsequently placed in a chamber with a mobile phase system of hexane and ethyl acetate in different ratios (7:3, 5:5, 9:1 v/v), ethyl acetate only, and methanol only. The separation of the substances was observed under visible light and Ultraviolet (UV) light at wavelengths of 254 nm and 365 nm. The Retention factor (Rf) for each spot was calculated using the following formula:

$$R_f = \frac{\text{Distance traveled by the component (cm)}}{\text{Distance traveled by mobile phase (cm)}}$$

The optimal mobile phase proportions for achieving the best compound separation were determined by the highest number of spots observed on the TLC plate's surface, which were then utilized for column chromatography (Omara et al. 2022).

Column chromatography

The bacterial crude extract was fractionated using column chromatography, following the method described by Chepkorir et al. (2018). A total of 45 g of silica gel 60 (0.063-0.2 mesh size) was mixed with hexane (10:0 v/v) and stirred to form a homogeneous slurry to pack the column. This slurry was then poured into a glass column containing a small amount of cotton and sand. Silica gel was gradually mixed with the bacterial crude extract until it became a fine green powder. The resulting sample mixture was loaded into the column and eluted with combinations of hexane, ethyl acetate, and methanol, establishing an increasing polarity gradient (0:10, 1:9, 3:7, 5:5, 7:3, 9:1, 10:0 v/v). The eluates from each mobile phase combination were collected and evaporated using a rotary evaporator at 50°C. Thereafter, the eluates were examined by TLC using hexane acetate (7:3 v/v) to determine similarities in their separation spots, and eluates exhibiting similar TLC profiles were combined into the same vial.

LC-MS/MS analysis

The chemical substances in the selected active fractions were identified using Liquid Chromatography-Tandem Mass Spectrometry (LC-MS/MS) with the Xevo G2-XS QTof (Waters, USA) and an Electrospray Ionization (ESI) interface. The separation was performed on a liquid chromatography system with the column maintained at 40°C. The samples were eluted over 17 minutes using a mobile phase composed of 0.1% formic acid in water (A) and acetonitrile (B) at a flow rate of 0.3 mL/min. Mass spectrometric data were collected in positive ion mode with a precursor m/z range of 100-1200. The source temperature was set to 120°C, and the capillary voltage was 2 kV. Furthermore, the composition and mass of each fragment and precursor ion were analyzed using data from the UNIFI software database (Septama et al. 2022).

Determination of the Minimum Inhibitory Concentration (MIC) of each bacterial metabolite fraction

The secondary metabolite fraction derived from the AJ5 strain underwent further assays to evaluate the MIC using a microdilution procedure (CLSI 2020). Briefly, microdilution was performed using Mueller-Hinton Broth (MHB) (Himedia, India) containing a fraction (100 µL) ranging from 5.63 µg/mL to 1880 µg/mL in 96 sterile well plates. Subsequently, the MRSA suspension (100 µL) at a density of 1×10^4 CFU/mL, was seeded into the wells (final MRSA concentration of 5×10^3 CFU/mL) and incubated overnight at 37°C. The MIC was established as the minimum concentration of extract that inhibited the visible growth of MRSA. Tetracycline (Merck, Germany) in the concentration ranged between 0.78 to 100 µg/mL), and methanol was used as positive and negative controls, respectively. According to Silva et al. (2013), antibacterial activity could be classified based on the MIC values of natural extracts. When the MIC value was less than 100 µg/mL, it was categorized as very strong, 100-500 µg/mL was considered strong, 500-1000 µg/mL was moderate, 1000-2000 µg/mL was weak, and above 2000 µg/mL was inactive.

Antibiofilm assay

The antibiofilm activity of selected active fractions was assessed through crystal violet staining in a 96-well plate, following CLSI (2020). A 100 µL suspension of MRSA at a concentration of 10^4 CFU/mL was added to Brain Heart Infusion (BHI) broth (Himedia, India) supplemented with 0.25% glucose. Different concentrations of the selected active fractions (1× MIC, ½× MIC, and ¼ ×MIC,) were inoculated into each well to achieve a final volume of 200 µL, then agitated at 150 rpm and 37°C for 24 hours. After incubation, the media and bacterial cells were removed twice using 0.85% NaCl solution, and 200 µL of 0.1% crystal violet was added to each well. The plate was incubated at 37°C for 30 minutes and then washed with 0.85% NaCl solution. The crystal violet-stained biofilm was dissolved in 200 µL of 99% DMSO. Its absorbance was measured using an ELISA microplate reader (Thermo Scientific Varioskan Flash, Massachusetts, USA) at 595 nm cell and the cell density of each well was also observed under a light microscope with a total magnification of 100×. MRSA cultures without treatment from the selected active fractions served as a control, while methanol (3.5% v/v) was used as a negative control. The percentage of suppression of biofilm formation was calculated using the following formula:

$$\text{Suppression of biofilm formation (\%)} = \frac{OD_{\text{negative control}} - OD_{\text{treatment}}}{OD_{\text{negative control}}} \times 100$$

Biofilm eradication assay

Around 200 µL of MRSA culture (1×10^4 CFU/mL) was inoculated into 96-well plates containing BHI medium and incubated for 5 days to promote mature biofilm formation. The medium was replaced daily with fresh BHI medium supplemented with 0.25% glucose. Furthermore, AJ5 fraction was added at concentrations of 1×MIC, ½×MIC, and ¼×MIC, and the plates were incubated for 24 hours at 37°C. After this incubation, the medium was removed, and the biofilm was stained with 10 µL of methyl tetrazolium solution (5 mg/mL) and incubated for 3 hours at 37°C. Following incubation, the samples were dissolved in 200 µL of 99% DMSO (Merk, Germany), and control was established using biofilm without any treatment. Absorbance was then measured using an ELISA reader (Varioskan Flash-Thermo Fisher, Thermo Scientific, Finland) at 595 nm, and the data were expressed as means±standard deviation from 3 replicates (Wintachai et al. 2019).

Data analysis

The experimental data from the antibiofilm assay and biofilm eradication test were collected in triplicate. This was then analyzed using One-Way Analysis of Variance

(ANOVA) and further examined with Tukey's analysis via Statistical Product and Service Solutions (SPSS) software version 29.0. Furthermore, a significance level of $p<0.05$ was set to determine statistical significance.

RESULTS AND DISCUSSION

Genome profile and identified Secondary Metabolite Gene Clusters (SMGCs) in *Priestia megaterium* AJ5

The complete genomic DNA of the AJ5 strain was successfully sequenced, resulting in a total assembled genome length of 5,750,510 base pairs (bp) with 99.35% genome completeness (Table 1). The average Guanine-Cytosine content (GC%) was 37.73%, and the total number of Coding Sequences (CDSs) was 6,016. Furthermore, the characteristic graphical map of the AJ5 genomic draft is shown in Figure 1. Based on Average Nucleotide Identity (ANI) analysis, the genomic sequences of the strain showed high similarity (ANI>98%) with *Priestia megaterium*, suggesting that this bacterium belonged to the same species (Table 2). The bacterium was closely related to *P. megaterium* NCTC10342, with an average ANI of 98.37%, followed by ATCC14581 (ANI: 98.36%), and NBRC15308 (ANI: 98.34%). The draft genome sequence of the AJ5 strain was accessible in the NCBI GenBank database under accession number CP170487. Furthermore, the SMGCs carried in the genomic draft of the AJ5 strain were identified. AntiSMASH analysis revealed that the bacterium had 5 types of SMGCs, including Non-Ribosomal Peptide Synthetase (NRPS)-Independent (NI) siderophores, 3 types of terpenes, and type III Polyketide Synthase (PKS) (Table 3). A total of 3 out of the 5 SMGCs found in the AJ5 genome were known to be involved in the synthesis of synechobactin C9, surfactin, and carotenoids. At the same time, the gene products of the other 2 identified gene types remain unidentified (Figure 2). Carotenoid secondary metabolite showed a high homology of 50%, while synechobactin C9 and surfactin exhibited low homologies (<40%).

Table 1. Genomic features of AJ5 strain

Genomic features	
Size of the genome assembly (bp)	5,750,510
GC content (%)	37.73
Number of contigs	6
Largest contig (bp)	5,134,075
Mean read length (bp)	24,831.6
Read length N50 (bp)	5,134,075
Coding sequences (CDSs)	6,016
Genome completeness (%)	99.35

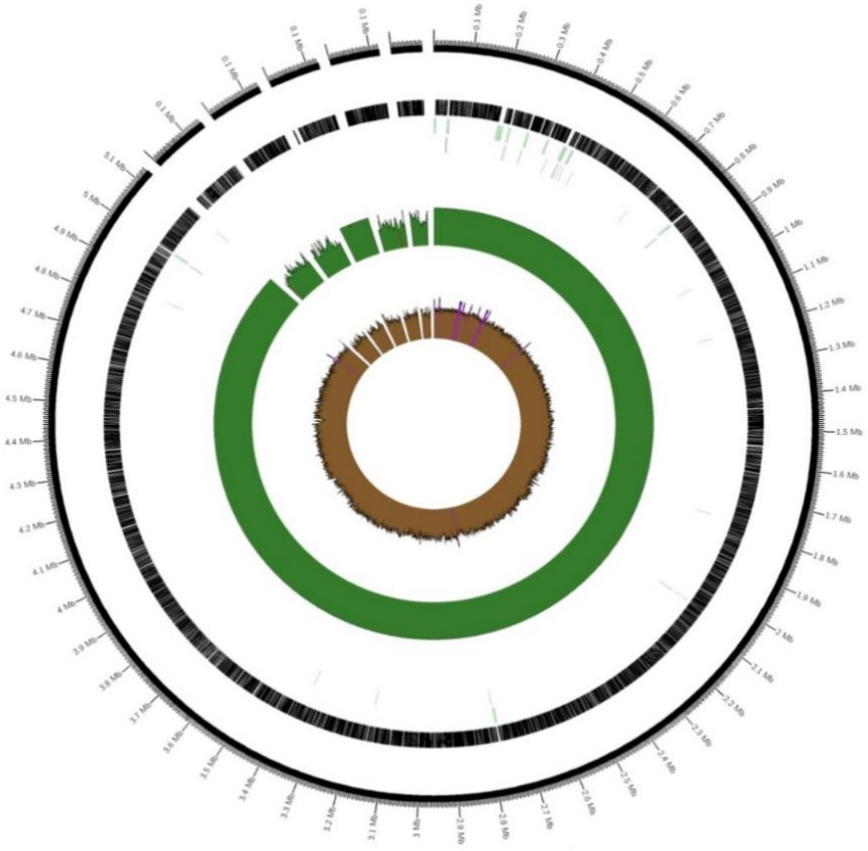

Figure 1. Visualization of whole genome AJ5 strain. Blue: Pseudogenes, black: CDS, green: rRNA, purple: tRNA, purple: gc content >50%, brown: gc content <50%. Total genome size 5,750,510 bp

Table 2. Selected closest relative strains of AJ5 strain based on whole genome sequences

Strain	Genus	Species	Genome size (Mb)	Genome accession number	ANI (%)
NCTC10342	*Priestia*	*P. megaterium*	5.8	GCA_900445485.1	98.37
ATCC14581	*Priestia*	*P. megaterium*	5.7	GCA_006094495.1	98.36
NBRC15308	*Priestia*	*P. megaterium*	5.5	GCA_001591525.1	98.34

Table 3. Putative Secondary Metabolite Gene Clusters (SMGCs) present in the genome of the AJ5 strain

Cluster	Length (bp)	Type	Compound	Bioactivity	Homology (%)	Source	References
Cluster 1	34,576	NRPS independent (NI)-siderophore	Synechobactin C9	Iron-chelator	23	*Synechococcus* sp. PCC 7002	Boiteau and Repeta (2015)
Cluster 2	20,819	Terpene	Surfactin	Antimicrobial	8	*Bacillus amyloliquefaciens* FZB42	Koumoutsi et al. (2004)
Cluster 3	20,849	Terpene	Carotenoid	Antioxidant	50	*Halobacillus halophilus* DSM 22	Köcher et al. (2009)
Cluster 4	21,869	Terpene	unidentified	-	-		-
Cluster 5	41,086	Type III PKS	unidentified	-	-		-

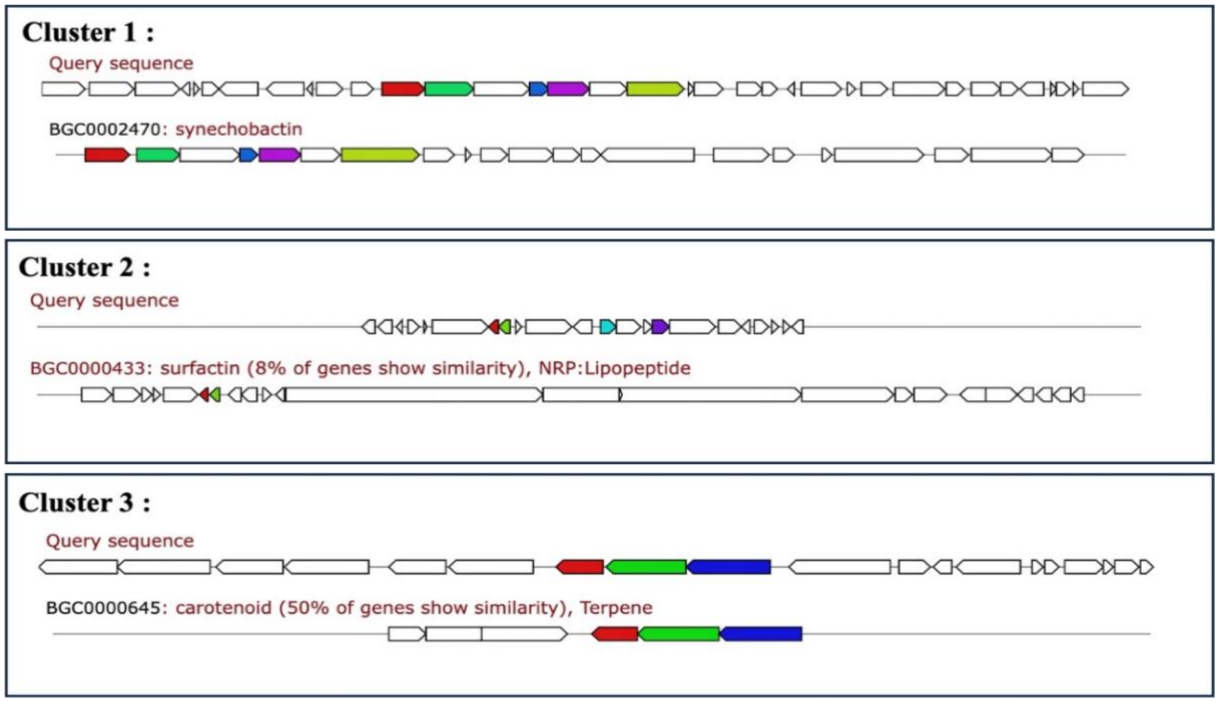

Figure 2. Comparison of Secondary Metabolite Gene Clusters (SMGCs) identified in the genome of AJ5 strain with those in the MIBiG database. Out of a total of 5 gene clusters, 3 were known to produce identified metabolites, while the products of the remaining 2 gene clusters remained unidentified

Secondary metabolite fractions, anti-MRSA activity, and their chemical profile

A total of 12 fractions were separated from the crude extract of the AJ5 strain through column chromatography (Table 4). Generally, these fractions showed a greenish-black spot on the TLC plate under UV light at λ 254 nm, differing in the number of spots separated. Compared to other fractions, F9 and F8 had a higher number of separated spots, while other fractions exhibited at least 2 spots. Additionally, the spot fractions displayed red, blue, and green spots under UV light at λ 365 nm (Figure 3). Furthermore, the Minimum Inhibitory Concentration (MIC) of all fractions was determined, revealing that these fractions had different MICs against MRSA (Table 5). F9, F12, and F8 exhibited the lowest MICs, categorized as strong anti-MRSA activity, with MICs of 117.5 µg/mL, 180 µg/mL, and 243.1 µg/mL, respectively. On the other hand, 2 fractions showed moderate activity, 5 fractions were considered weak, and 2 fractions were inactive. The 2 best fractions (F9 and F12) were then selected for further identification and antibiofilm analysis.

LC-MS/MS-based identification showed that both F9 and F12 had different chemical profiles (Figure 4). Nevertheless, nigakilactone H was found in both fractions, and each had other distinct components with varying retention times and abundances. F9 contained tetratriacontanamine and 2 other unidentified compounds, while F12 contained 2-(p-Anisyl)-5-methyl-1-hexene and 3 other unidentified compounds.

Biofilm suppression and eradication of Nigakilactone H-containing fractions

A total of 2 selected fractions, F9 and F12, demonstrated promising antibiofilm activity, as indicated by their ability to suppress biofilm formation of MRSA. Briefly, the F9 fraction was more active than F12, with F9 capable of inhibiting MRSA biofilm formation by up to 81.54±1.80% at the 1×MIC treatment (Figure 5). The inhibition of biofilm formation was not significantly different among the treatments with 1×MIC, 1/2xMIC, and 1/4×MIC. On the other hand, F12 was also capable of suppressing biofilm formation by up to 77.01±1.96%. There were no significant differences between the treatments with 1×MIC and 1/4×MIC, but these treatments were significantly different from the 1/2×MIC treatment. In addition, cell density stained with crystal violet was also higher in control, compared to treatments. MRSA cell density decreased following higher concentration of fractions (Figure 6).

The F9 and F12 fractions also exhibited a dose-dependent eradication effect on mature MRSA biofilm. The highest eradication effects of F9 and F12 fractions were observed at a concentration of 1×MIC, with eradication percentages of 79.23±1.96% and 58.89±1.07%, respectively. Therefore, the F9 fraction had a stronger eradication effect than the F12 fraction, and this decreased as the fraction concentration was reduced (Figure 7).

Discussion

Microbial natural products derived from endophytic bacteria represent a vast source of potential future drugs for pharmaceutical applications. Bacterial genome mining aids in the discovery and identification of both characterized and uncharacterized SMGCs, facilitating the exploration of novel SMGCs. This study conducted whole genome sequencing and bioinformatics analyses to predict gene clusters responsible for the biosynthesis of these compounds, and to investigate the capability of the AJ5 strain in synthesizing secondary metabolites. In a previous study, 16S rRNA-based identification revealed that the AJ5 strain was highly similar to *Priestia megaterium* ATCC 14581 (accession no. NR_116873.1) (Priyanto et al. 2023). Confirming this result, the complete genome sequence (total length: 5,750,510 bp, with 99.35% genome completeness) further validated the identity of the strain. The AJ5 strain exhibited the highest similarity to *P. megaterium* NCTC 10342 (accession no. GCA_900445485.1), with a high ANI of 98.37%, followed closely by *P. megaterium* ATCC 14581 and *P. megaterium* NBRC 15308, with ANIs of 98.36% and 98.34%, respectively. These values confirmed that the bacterium belonged to the same species, as the average cutoff was greater than 95% (Yoon et al. 2017). This species was widely distributed in various environments, including soil (Adeniji et al. 2024), plant tissue (Jo et al. 2023), marine environments (Tay et al. 2023), and chicken manure (Deng et al. 2021), highlighting its potential for various biotechnological applications.

Table 4. Purified fraction derived from secondary metabolite AJ5 strain using 3 different mobile phases

Fraction code	Mobile phase	Weight (mg)
F1	Hexane:ethyl acetate (7:3 v/v)	37.0
F2	Hexane:ethyl acetate (7:3 v/v)	64.7
F3	Hexane:ethyl acetate (7:3 v/v)	61.0
F4	Hexane:ethyl acetate (7:3 v/v)	26.6
F5	Hexane:ethyl acetate (5:5 v/v)	43.7
F6	Hexane:ethyl acetate (5:5 v/v)	61.0
F7	Hexane:ethyl acetate (9:1 v/v)	50.6
F8	Ethyl acetate	74.6
F9	Ethyl acetate	68.9
F10	Ethyl acetate	42.0
F11	Methanol	69.0
F12	Methanol	24.2

Table 5. Minimum Inhibitory Concentration (MIC) of fractions from AJ5 strain against MRSA

Fraction	MIC (µg/mL)	Effectivity
F1	>1005	Weak
F2	1585	Weak
F3	>2240	Inactive
F4	980	Moderate
F5	>1190	Weak
F6	867.5	Moderate
F7	>1625	Weak
F8	243.1	Strong
F9	117.5	Strong
F10	>1320	Weak
F11	>2490	Inactive
F12	180	Strong
Tetracycline	6.25	Very strong

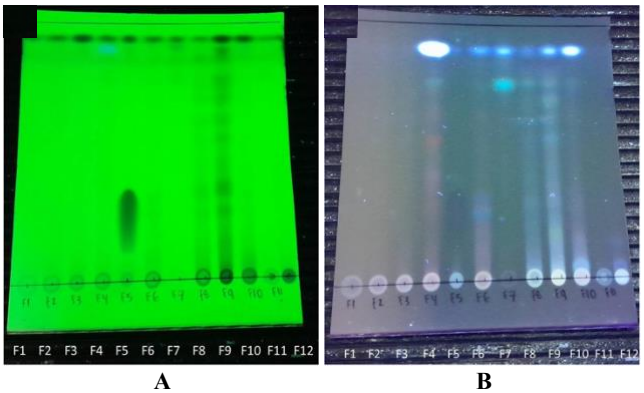

A B

Figure 3. Spot profile of 12 fractions derived from AJ5 strain in TLC plate using mobile phase hexane: Ethyl acetate (7:3 v/v) observed under ultraviolet light at a wavelength: A. 254 nm, and B. 365 nm

The AntiSMASH analysis was applied to screen SMGCs present in the AJ5 genome sequences. These bioinformatics tools suggested that a genomic draft of the bacterium possessed possible 5 SMGCs, such as Non-Ribosomal Peptide Synthetase (NRPS)-Independent (NI) siderophores, 3 types of terpenes, and type III PKS. A total of 3 out of 5 gene clusters were known to be responsible for the biosynthesis of bio compounds, including synecobactin C9, surfactin, and carotenoid. Overall identified secondary metabolites showed low homologies (<40%), except carotenoid (homology: 50%), likely suggesting the novelty of the genes and gene products. Synecobactin was a siderophore that was well known to be synthesized by cyanobacteria via NRPS independent pathway. In comparison, most siderophores were synthesized through the NRPS pathway, usefull for bioremediation and medicinal application (Årstøl and Hohmann-Marriott 2019). Synecobactin-related gene was also found in the genome of *P. megaterium* MARUCO02 isolated from mangrove sediments (Maghembe et al. 2023). In addition, the AJ5 genome also contained SMGCs for surfactin, a lipopeptide antibiotic that commonly produced by *Bacillus* species. Surfactin, derived from endophytic *B. amyloliquefaciens* strain RKEA3, exhibited a remarkable antibacterial property against *S. aureus* (Rasiya and Sebastian 2021). Moreover, the AJ5 genome also contained gene clusters that were 50% similar to the gene cluster responsible for carotenoid biosynthesis. The substance was important for the self-protection of this bacterium from UV radiation and oxidative stresses (Hartz et al. 2018). Earlier studies proved that microbial carotenoids showed strong antibacterial activity against MRSA and MDR *Escherichia coli* (Kusmita et al. 2023). However, AJ5 strain genome also carried 2 other gene clusters with unidentified natural products, indicating an opportunity for further investigation to find novel compounds. Generally, antiSMASH analysis of AJ5 strain revealed its potential biosynthetic pathway of secondary metabolites valuable for pharmaceutical purposes.

Fractionation was an important procedure for purifying secondary metabolites from natural sources. In this study, TLC and column chromatography were employed to obtain more purified compounds produced by the AJ5 strain. A total of 12 fractions with different R_f and spot characteristics were successfully isolated. All fractions were subjected to a microbroth dilution assay to investigate the active fractions' function against MRSA. Each fraction differed in anti-MRSA activities, as indicated by their MICs. A total of 2 fractions, F9 and F12, with MICs less than 200 µg/mL, were selected for further identification and antibiofilm assays, as these could significantly contribute to the anti-MRSA effect of the extract. These selected fractions contained nigakilactone H, a triterpenoid previously reported in plants such as *Picrasma quassioides* (D.Don) Benn. (NCBI 2024). Nigakilactone H-containing fractions isolated from *Hibiscus sabdariffa* L. had shown cytotoxic effects against breast cancer cell lines (Yuliastri et al. 2022). However, no previous studies had reported its antimicrobial activity. Further purification was necessary to isolate and investigate further its role in antibacterial properties. Other compounds identified in the selected fractions included tetratriacontanamine and 2-(p-anisyl)-5-methyl-1-hexene, which had also not been previously reported as antibacterial agents. Additionally, 2 compounds in the F9 fraction and 2 compounds in the F12 fraction remained unidentified, suggesting that other approaches were necessary to characterize these compounds. To our knowledge, this was the first report that the nigakilactone H-containing fraction displayed anti-MRSA activity.

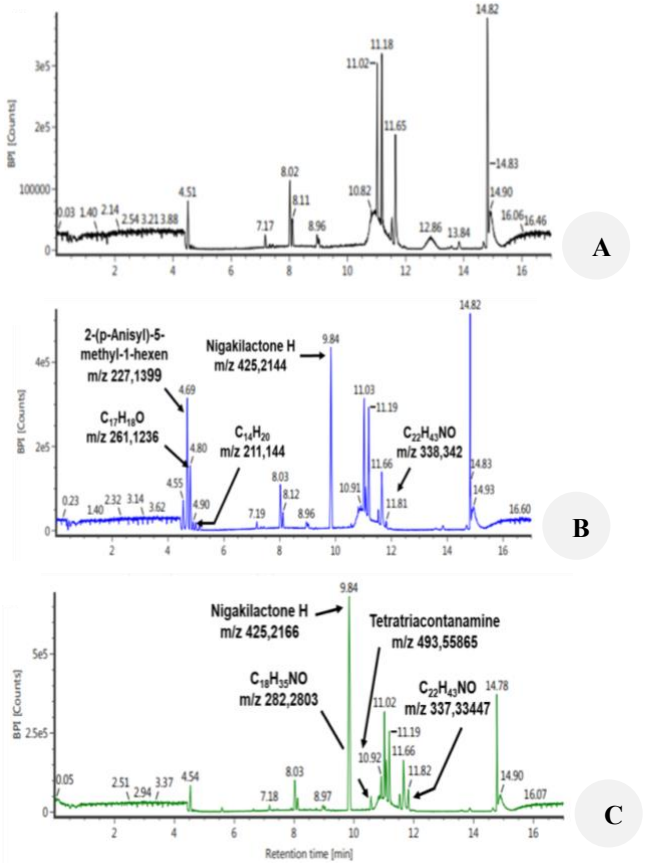

Figure 4. Chromatogram profile of: A. Blank, B. F12, and C. F9 fractions analyzed using LC-MS/MS

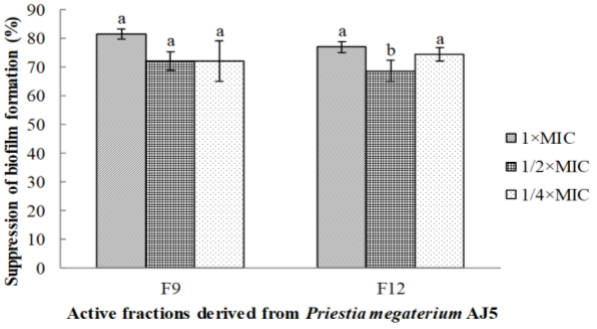

Figure 5. Suppression of biofilm formation was demonstrated by 2 selected active fractions from the secondary metabolites of the AJ5 strain. Different letters above the bars for each fraction treatment indicated statistically significant differences (P<0.05)

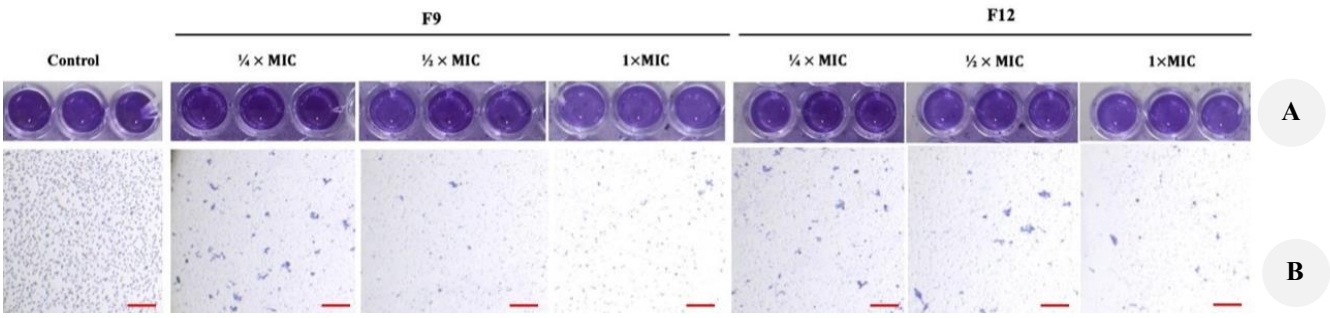

Figure 6. Reduction of MRSA cell density following the increase of fraction concentration. A. Well after it was stained with crystal violet, B. MRSA cell population was observed under a compound microscope with a total magnification of 100×. Red bars represent 100 µm

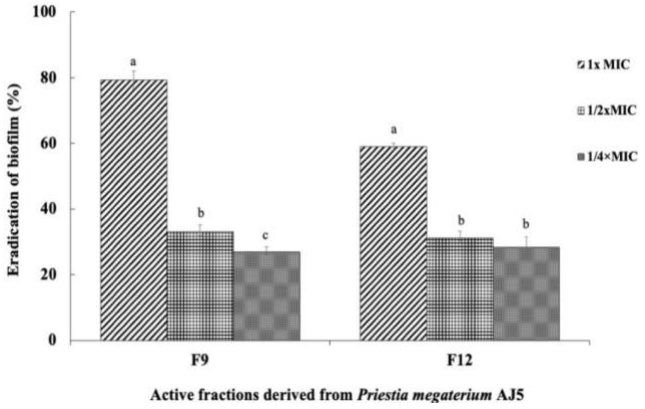

Figure 7. Biofilm eradication effect of active fractions from *Priestia megaterium* AJ5. Different letters above the bars for each fraction treatment indicate statistically significant differences ($P<0.05$)

Biofilm significantly contributed to preventing the penetration of antimicrobial substances into bacterial cells, resulting in drug resistance that was 10 to 1,000 times greater than in their planktonic forms (Tuon et al. 2023). This study revealed that the 2 selected fractions exhibited a remarkable suppressive effect on biofilm formation in MRSA. Treatment with ¼ ×MIC (29.38 µg/mL), ½ ×MIC (58.75 µg/mL), and 1×MIC (117.5 µg/mL) of the F9 fraction was capable of suppressing MRSA biofilm formation by up to 81.54% (with no statistically significant differences among the treatments). In comparison, the F12 fraction inhibited up to 77% of biofilm formation. Following this study, a purified peptide from a *Brevibacillus* strain showed 50% inhibition of MRSA biofilm at 2.92 µg/mL and completed biofilm inhibition at 128 µg/mL (Ogunsile et al. 2023). Supporting this study, a metallopeptidase-producing *Priestia* strain isolated from a marine sponge also demonstrated antibiofilm properties against *S. aureus*, achieving up to 92% inhibition (Ribeiro et al. 2024). These 2 fractions also eradicated established biofilms in a dose-dependent manner, with higher eradication activity observed at higher fraction concentrations. At a concentration of 1× MIC, the F9 and F12 fractions eradicated MRSA biofilm by 79.23±1.96% and 58.89±1.07%, respectively. The eradication activity decreased with a reduction in fraction concentration, indicating that the variability in response to antibiofilm activity depended on metabolite concentration. The effectiveness of each fraction in eradicating mature biofilms was lower than its activity in inhibiting biofilm formation. This suggests that established biofilms hinder the penetration of antimicrobial substances, therefore reducing their effectiveness.

In conclusion, this study investigated the genomic profile of the endophytic bacterium AJ5 strain, along with in vitro assays assessing its antibiofilm potential against MRSA. The complete genome sequence of this bacterium confirmed a high similarity to *P. megaterium*. The bacterial genome also contained 5 SMGCs potentially involved in the biosynthesis of secondary metabolites. Discovery of 2 active fractions which exhibited strong antibacterial and antibiofilm activities against MRSA, was a significant breakthrough. These fractions contained contain nigakilactone H, along with other distinct components such as tetratriacontanamine and 2-(p-Anisyl)-5-methyl-1-hexene. This study was the first to demonstrate the inhibitory effects of these compounds on MRSA growth and biofilm formation, potentially paving the way for novel antibacterial strategies. The unidentified compounds in each fraction present an exciting avenue for future research, inspiring further exploration in the field. Unidentified compounds presented in each fraction warrant further investigation in future studies. Therefore, a subsequent study should focus on the identification and purification of individual compounds and the exploration of their antibacterial mechanisms, particularly those of nigakilactone H, in order to discover more promising substances compared to the existing active compounds. Additionally, investigating the biosynthetic pathways of known metabolites is essential. This preliminary study underscored the anti-MRSA potential of the AJ5 strain, which could serve as a valuable source for the development of anti-MRSA compounds in the future.

ACKNOWLEDGEMENTS

This study was fully funded by the Directorate of Research and Innovation, Bogor Agricultural University (IPB University), Bogor, Indonesia, through the Young Lecturer

Research Program/*Program Penelitian Dosen Muda* 2024 (grant number: 23427/IT3/PT.01.03/P/B/2024).

REFERENCES

Adeniji AA, Ayangbenro AS, Babalola OO. 2024. Draft genome sequence of *Priestia megaterium* AB-S79 strain isolated from active gold mine. Microbiol Resour Announc 13: e0105523. DOI: 10.1128/mra.01055-23.

Alberus JY, Verdel-Aranda K, Martinez-Hernandez A, de Jesús Yañez-Morales M, Lara-Reyna J. 2022. Genome mining for bioprospecting of biosynthetic genes clusters for bacterial metabolites potentially useful in agroecological production. Agro Productividad 15 (9): 77-87. DOI: 10.32854/agrop.v15i9.2226.

Alghamdi BA, Al-Johani I, Al-Shamrani JM, Alshamrani HM, Al-Otaibi BG, Almazmomi K, Yusof NY. 2023. Antimicrobial resistance in methicillin-resistant *Staphylococcus aureus*. Saudi J Biol Sci 30 (4): 103604. DOI: 10.1016/j.sjbs.2023.103604.

Al-Theyab NS, Abuelizz HA, Al-Hamoud GA, Aldossary A, Liang M. 2023. *Priestia megaterium* metabolism: Isolation, identification of naringenin analogues and genes elevated associated with nanoparticle intervention. Curr Issues Mol Biol 45 (8): 6704-6716. DOI: 10.3390/cimb45080424.

Al-Thubiani ASA, Maher YA, Fathi A, Abourehab MAS, Alarjah M, Khan MSA, Al-Ghamdi SB. 2018. Identification and characterization of a novel antimicrobial peptide compound produced by *Bacillus megaterium* strain isolated from oral microflora. Saudi Pharm J 26 (8): 1089-1097. DOI: 10.1016/j.jsps.2018.05.019.

Andrzejczuk S, Cygan M, Dłuski D, Stępień-Pyśniak D, Kosikowska U. 2023. Staphylococcal resistance patterns, *blaZ* and SCC *mec* cassette genes in the nasopharyngeal microbiota of pregnant women. Intl J Mol Sci 24 (9): 7980. DOI: 10.3390/ijms24097980.

Årstøl E, Hohmann-Marriott MF. 2019. Cyanobacterial siderophores-physiology, structure, biosynthesis, and applications. Mar Drugs 17 (5): 281. DOI: 10.3390/md17050281.

Belknap KC, Park CJ, Barth BM, Andam CP. 2020. Genome mining of biosynthetic and chemotherapeutic gene clusters in *Streptomyces* bacteria. Sci Rep 10 (1): 2003. DOI: 10.1038/s41598-020-58904-9.

Blin K, Shaw S, Augustijn HE, Reitz ZL, Biermann F, Alanjary M, Fetter A, Terlouw BR, Metcalf WW, Helfrich EJN, van Wezel GP, Medema MH, Weber T. 2023. AntiSMASH 7.0: New and improved predictions for detection, regulation, chemical structures and visualisation. Nucleic Acids Res 51 (W1): W46-W50. DOI: 10.1093/nar/gkad344.

Boiteau RM, Repeta DJ. 2015. An extended siderophore suite from *Synechococcus* sp. PCC 7002 revealed by LC-ICPMS-ESIMS. Metallomics 7 (5): 877-884. DOI: 10.1039/c5mt00005j.

Chepkorir R, Matasyoh JC, Wagara IN. 2018. Two withanolides from *Withania somnifera* (Solanaceae) and activity of methanolic extracts against fungal and bacterial pathogens that affects food crops. Afr J Food Sci 12 (5): 115-125. DOI: 10.5897/ajfs2016.1503.

Christina A, Christapher V, Bhore SJ. 2013. Endophytic bacteria as a source of novel antibiotics: An overview. Pharmacogn Rev 7 (13): 11-16. DOI: 10.4103/0973-7847.112833.

Clinical and Laboratory Standars Institute (CLSI). 2020. Performance Standards for Antimicrobial Susceptibility Testing. Clinical and Laboratory Standards Institute, Pennsylvania.

Cui Z, Hu L, Zeng L, Meng W, Guo D, Sun L. 2023. Isolation and characterization of *Priestia megaterium* KD7 for the biological control of pear fire blight. Front Microbiol 14: 1099664. DOI: 10.3389/fmicb.2023.1099664.

Deng B, Wang L, Ma Q, Yu T, Liu D, Dai Y, Zhao G. 2021. Genomics analysis of *Bacillus megaterium* 1259 as a probiotic and its effects on performance in lactating dairy cows. Animals 11 (2): 397. DOI: 10.3390/ani11020397.

Flemming HC, Wuertz S. 2019. Bacteria and Archaea on earth and their abundance in biofilms. Nat Rev Microbiol 17 (4): 247-260. DOI: 10.1038/s41579-019-0158-9.

Hartz P, Milhim M, Trenkamp S, Bernhardt R, Hannemann F. 2018. Characterization and engineering of a carotenoid biosynthesis operon from *Bacillus megaterium.* Metab Eng 49: 47-58. DOI: 10.1016/j.ymben.2018.07.017.

Hwang H-H, Chien P-R, Huang F-C, Yeh P-H, Hung S-HW, Deng W-L, Huang C-C. 2022. A plant endophytic bacterium *Priestia megaterium* strain BP-R2 isolated from the halophyte *Bolboschoenus planiculmis* enhances plant growth under salt and drought stresses. Microorganisms 10: 2047. DOI: 10.3390/microorganisms10102047.

Jo HW, Lim K, Ibal JC, Kim M-C, Kim H-B, Baek C, Heo YM, Lee H, Kang S, Lee D-G, Shin J-H. 2023. Growth increase in the herbaceous plant *Centella asiatica* by the plant growth-promoting rhizobacteria *Priestia megaterium* Hyang Yak-01. Plants 12 (13): 2398. DOI: 10.3390/plants12132398.

Khan HA, Baig FK, Mehboob R. 2017. Nosocomial infections: Epidemiology, prevention, control and surveillance. Asian Pac J Trop Biomed 7 (5): 478-482. DOI: 10.1016/j.apjtb.2017.01.019.

Kim MS, Jeong D-E, Jang J-P, Jang J-H, Choi S-K. 2024. Mining biosynthetic gene clusters in *Paenibacillus* genomes to discover novel antibiotics. BMC Microbiol 24 (1): 226. DOI: 10.1186/s12866-024-03375-5.

Köcher S, Breitenbach J, Müller V, Sandmann G. 2009. Structure, function and biosynthesis of carotenoids in the moderately halophilic bacterium *Halobacillus halophilus*. Arch Microbiol 191 (2): 95-104. DOI: 10.1007/s00203-008-0431-1.

Koumoutsi A, Chen X-H, Henne A, Liesegang H, Hitzeroth G, Franke P, Vater J, Borriss R. 2004. Structural and functional characterization of gene clusters directing non-ribosomal synthesis of bioactive cyclic lipopeptides in *Bacillus amyloliquefaciens* strain FZB42. J Bacteriol 186 (4): 1084-1096. DOI: 10.1128/JB.186.4.1084-1096.2004.

Kusmita L, Edi ANP, Franyoto YD, Mutmainah, Haryanti S, Nurcahyanti ADR. 2023. Sun protection and antibacterial activities of carotenoids from the soft coral *Sinularia* sp. symbiotic bacteria from Panjang Island, North Java Sea. Saudi Pharm J 31 (8): 101680. DOI: 10.1016/j.jsps.2023.06.013.

Maghembe RS, Mdoe FP, Makaranga A, Mpemba JA, Mark D, Mlay C, Moto EA, Mtewa AG. 2023. Complete genome sequence data of *Priestia megaterium* strain MARUCO02 isolated from marine mangrove-inhabited sediments of the Indian Ocean in the Bagamoyo Coast. Data Brief 48: 109119. DOI: 10.1016/j.dib.2023.109119.

Mahmoud FM, Kusari S, Kublik S, Benning S, Siani R, Zühlke S, Radl V, Mahnkopp-Dirks F, Schloter M. 2023. Draft genome sequence of the bacterial endophyte *Priestia megaterium* B1, isolated from roots of apple (*Malus domestica*). Microbiol Resour Announc 12 (6): e0117222. DOI: 10.1128/mra.01172-22.

Malanicheva IA, Kozlov DG, Sumarukova IG, Efremenkova OV, Zenkova VA, Katrukha GS, Reznikova MI, Tarasova OD, Sineokii SP, El'-Registan GI. 2012. Antimicrobial activity of *Bacillus megaterium* strains. Microbiology 81: 178-185. DOI: 10.1134/s0026261712020063.

Montravers P, Eckmann C. 2021. Cotrimoxazole and clindamycin in skin and soft tissue infections. Curr Opin Infect Dis 34 (2): 63-71. DOI: 10.1097/qco.0000000000000698.

Murray CJL, Ikuta KS, Sharara F et al. 2022. Global burden of bacterial antimicrobial resistance in 2019: A systematic analysis. Lancet 399 (10325): 629-655. DOI: 10.1016/S0140-6736(21)02724-0.

National Center for Biotechnology Information (NCBI). 2024. PubChem Compound Summary for CID 467797, Nigakilactone H. https://pubchem.ncbi.nlm.nih.gov/compound/Nigakilactone-H.

Ogunsile A, Songnaka N, Sawatdee S, Lertcanawanichakul M, Krobthong S, Yingchutrakul Y, Uchiyama J, Atipairin A. 2023. Anti-methicillin-resistant *Staphylococcus aureus* and antibiofilm activity of new peptides produced by a *Brevibacillus* strain. PeerJ 11: e16143. DOI: 10.7717/peerj.16143.

Omara T, Kiprop AK, Kosgei VJ. 2022. Isolation and characterization of compounds in ethanolic extract of *Albizia coriaria* (Welw ex. Oliver) leaves: A further evidence of its ethnomedicinal diversity. Bull Natl Res Cent 46: 30. DOI: 10.1186/s42269-022-00716-0.

Priyanto JA, Prastya ME, Astuti RI, Kristiana R. 2023. The antibacterial and antibioflm activities of the endophytic bacteria associated with *Archidendron pauciforum* against multidrug-resistant strains. Appl Biochem Biotech 195 (11): 6653-6674. DOI: 10.1007/s12010-023-04382-4.

Priyanto JA, Prastya ME, Hening ENW, Suryanti E, Kristiana R. 2024. Two strains of endophytic *Bacillus velezensis* carrying antibiotic-biosynthetic genes show antibacterial and antibiofilm activities against Methicillin-Resistant *Staphylococcus aureus* (MRSA). Indian J Microbiol 64 (4): 1884-1893. DOI: 10.1007/s12088-024-01262-1.

Rasiya KT, Sebastian D. 2021. Iturin and surfactin from the endophyte *Bacillus amyloliquefaciens* strain RKEA3 exhibits antagonism against *Staphylococcus aureus.* Biocatal Agric Biotechnol 36: 102125. DOI: 10.1016/j.bcab.2021.102125.

Ribeiro NS, da Rosa DF, Xavier MA, dos Reis SV, Beys-da-Silva WO, Santi L, Bizarro CV, Dalberto PF, Basso LA, Macedo AJ. 2024. Unveiling antibiofilm potential: Proteins from *Priestia* sp. targeting *Staphylococcus aureus* biofilm formation. Antonie van Leeuwenhoek 117 (1): 78. DOI: 10.1007/s10482-024-01977-7.

Saikat TA, Khan MAS, Islam MS, Tasnim Z, Ahmed S. 2024. Characterization and genome mining of *Bacillus subtilis* BDSA1 isolated from river water in Bangladesh: A promising bacterium with diverse biotechnological applications. Heliyon 10 (14): e34369. DOI: 10.1016/j.heliyon.2024.e34369.

Septama AW, Tasfyati AN, Kristiana R, Jaisi A. 2022. Chemical profles of essential oil from Javanese turmeric (*Curcuma xanthorrhiza* Roxb.): Evaluation of its antibacterial and antibioflm activities against selected clinical isolates. S Afr J Bot 146: 728-734. DOI: 10.1016/j.sajb.2021.12.017.

Shi L, Zhu X, Qian T, Du J, Du Y, Ye J. 2023. Mechanism of salt tolerance and plant growth promotion in *Priestia megaterium* ZS-3 revealed by cellular metabolism and whole-genome studies. Intl J Mol Sci 24 (21): 15751. DOI: 10.3390/ijms242115751.

Silva ACO, Santana EF, Saraiva AM, Coutinho FN, Castro RHA, Pisciottano MNC, Amorim ELC, Albuquerque UP. 2013. Which approach is more effective in the selection of plants with antimicrobial activity?. Evid Based Complement Alternat Med 2013: 308980. DOI: 10.1155/2013/308980.

Silva V, Almeida L, Gaio V, Cerca N, Manageiro V, Caniça M, Capelo JL, Igrejas G, Poeta P. 2021. Biofilm formation of multidrug-resistant MRSA strains isolated from different types of human infections. Pathogens 10 (8): 970. DOI: 10.3390/pathogens10080970.

Tamang P, Upadhaya A, Paudel P, Meepagala K, Cantrell CL. 2024. Mining biosynthetic gene clusters of *Pseudomonas vancouverensis* utilizing whole genome sequencing. Microorganisms 12 (3): 548. DOI: 10.3390/microorganisms12030548.

Tay DD, Choo M-Y, Musa SM, Ahmad HF. 2023. Whole genome sequencing of *Priestia megaterium* isolated from the gut of sea cucumber (*Holothuria leucospilota*). Mater Today: Proc 75 (Part 1): 123-126. DOI: 10.1016/j.matpr.2022.10.150.

Tuon FF, Suss PH, Telles JP, Dantas LR, Borges NH, Ribeiro VST. 2023. Antimicrobial treatment of *Staphylococcus aureus* biofilms. Antibiotics 12 (1): 87. DOI: 10.3390/antibiotics12010087.

Vestergaard M, Frees D, Ingmer H. 2019. Antibiotic resistance and the MRSA problem. Microbiol Spectr 7: 10.1128/microbiolspec.gpp3-0057-2018. DOI: 10.1128/microbiolspec.gpp3-0057-2018.

Wintachai P, Paosen S, Yupanqui CT, Voravuthikunchai SP. 2019. Silver nanoparticles synthesized with *Eucalyptus critriodora* ethanol leaf extract stimulate antibacterial activity against clinically multidrug-resistant *Acinetobacter baumannii* isolated from pneumonia patients. Microb Pathog 126: 245-257. DOI: 10.1016/j.micpath.2018.11.018.

Yoon S-H, Ha S-M, Lim J, Kwon S, Chun J. 2017. A large-scale evaluation of algorithms to calculate average nucleotide identity. Antonie Van Leeuwenhoek 110 (10): 1281-1286. DOI: 10.1007/s10482-017-0844-4.

Yuliastri WO, Diantini A, Ghozali M, Sahidin I, Isrul M. 2022. Phytochemical constituent and in-vitro cytotoxic activity of *Hibiscus sabdariffa* L. calyx fraction on human breast cancer cell line mda-mb-231. Rasayan J Chem 15: 1619-1625. DOI: 10.31788/RJC.2022.1536694.

Zhang X, Zhang D, Ding Y, Li Z, Wang C, Ye S. 2023. Biosynthesis of resveratrol by an endophytic *Priestia megaterium* PH3 via the phenylpropane pathway. Appl Microbiol Biotechnol 107 (24): 7581-7599. DOI: 10.1007/s00253-023-12768-x.